

# Fast Alignment of Limited Angle Tomograms by projected Cross Correlation

Ricardo M. Sánchez<sup>\*†</sup>, Rudolf Mester<sup>‡§</sup>, Mikhail Kudryashev<sup>\*†</sup>

<sup>\*</sup>Max Planck Institute for Biophysics, Frankfurt am Main, Germany

<sup>†</sup>Buchmann Institute for Molecular Life Sciences, Goethe University, Frankfurt am Main, Germany

<sup>‡</sup>Visual Sensorics & Inf. Proc. Lab, Goethe University, Frankfurt am Main, Germany

<sup>§</sup>Norwegian Open AI Lab, CS Dept. (IDI), NTNU Trondheim, Norway

**Abstract**—Volume alignment is a computationally intensive task. In Subtomogram Averaging (StA) from electron cryotomograms (CryoET), thousands of *subtomograms* are aligned to a reference, which may take hours until days of computational time. CryoET datasets contain a limited number of noisy projections, with very low signal-to-noise ratio (SNR). The noisy subtomograms are aligned to a reference using cross-correlation, an operation that can be optimized when working with limited angle tomograms (LAT), as they are sparse in Fourier space.

We propose a *projected cross-correlation (pCC)* algorithm, a faster approach to computing the cross-correlation between a *limited angle (sub)-tomogram* and a given reference, and we use pCC to design a new procedure for volume alignment. pCC employs the projections to calculate the cross-correlation with lower computational complexity, as it works with a set of 2D projections instead of volumes. With this, we propose the *Substacks Averaging (SsA)* method as an alternative to the conventional Subtomogram Averaging (StA).

Our results on test data shows that SsA is considerably faster than the reference StA implementation: for 41 projections ( $k = 41$ ) and  $N = 200$ , the SsA is 35 times faster, and for  $N = 320$ , is 150 times faster. Furthermore, SsA results in higher precision of alignment of subtomograms at different noise levels.

## I. INTRODUCTION

Cryo electron tomography (CryoET) is an imaging technique superior in visualizing biological macromolecules in near-native context [1]. Biological samples are fixed in vitreous ice and are imaged in an electron microscope at different angles to obtain a set of two-dimensional projections, typically over a range of  $120^\circ$  with steps of few degrees, resulting in 41 to 61 images. Furthermore, the total electron dose used to record the tomogram is limited, as it damages the sample to be imaged, and it has to be distributed among all projections. This reduces the number of projections that can be acquired and lowers the signal-to-noise ratio (SNR) of each of them. The reconstructed tomograms suffer from elongations caused by the limited acquisition range, minor artifacts appear due to the angular steps, and the level of noise is high.

Multiple copies of the target macromolecule can be found in tomograms in different orientations. The Subtomogram Averaging (StA) approach [2], [3] aligns subtomograms, small 3D blocks of the tomogram, containing copies of the same target macromolecule to a common reference and sums them together to reduce the noise, to compensate for the missing views, and to obtain higher resolution volumes. Subtomogram alignment is an exhaustive 3D-rotational and 3D-translational

search to find the transformation parameters between the noisy limited angle subtomograms and a less noisy fully sampled reference. Constrained cross-correlation is used as a similarity metric. The StA technique is computational intensive, as it has to iteratively align thousands of subtomograms to one or multiple references.

Here we propose an alternative way to calculate the cross-correlation and improve the computational performance of the subtomogram alignment of limited angle tomograms. Instead of using a subtomogram and a reference, we use the substack, or set of projections used to reconstruct the subtomogram, to calculate the 3D cross-correlation. As the subtomograms come from a limited number of projections, the computational complexity is reduced. In the conventional StA algorithm, the alignment part requires  $O(N^3)$  operations, where  $N$  is the side length of the subtomogram, while the proposed algorithm requires only  $O(kN^2)$  operations, where  $k$  is the number of projections. We furthermore add a  $l_1$  regularization term to the cross-correlation, which further improves its accuracy. Our tests show that, for a typical subtomogram averaging dataset, our algorithm gives a significant speedup and an increment of the precision of the alignment.

## A. Related Work

A similar approach was proposed by the technique called Projection-Based Volume Alignment (PBVA) [4]. It is slightly faster than our approach, as it approximates the cross-correlation instead of calculating it. However, for the same reason, the precision of the alignment is limited. We compare the accuracy and precision of our proposed approach to PBVA.

StructS-XCorr [5] also uses projections and the  $l_1$  regularization penalty to improve the cross-correlation, as it is sparse in real space, and it applies it to find the delay between audio signals. Even though some ideas and conclusions are similar to our approach, its motivation and final applications are different. StructS-XCorr uses random projections to get the random sampling of compressive sensing and the  $l_1$  regularization penalty to reconstruct the cross-correlation. In our approach, we use the limited number of projections used in CryoET, and the  $l_1$  regularization as an optional cross-correlation enhancement.

## II. CROSS-CORRELATION FOR LIMITED ANGLE TOMOGRAMS

The traditional procedure to calculate the cross-correlation is to reconstruct the limited angle tomogram and then cross-correlate it to a reference volume, this operation performed in Fourier space. The cross-correlation  $\varphi_{v_1, v_2}$  is defined as follows: given two volumes,  $v_1$  and  $v_2$ , their Fourier transforms  $V_1 = \mathcal{F}v_1$  and  $V_2 = \mathcal{F}v_2$ , the element-wise multiplication operator  $\odot$ , and  $\bar{V}_2$ , the complex conjugate of  $V_2$ , then:

$$\varphi_{v_1, v_2} = \mathcal{F}^{-1}(V_1 \odot \bar{V}_2). \quad (1)$$

We must note that in limited angle tomography the Fourier space is not fully covered (sparse), which turns most of the element-wise multiplications into multiplications-by-0. We use the *Fourier central slice theorem* and the *direct Fourier reconstruction method* to calculate the cross-correlation that takes advantage of this sparsity.

The *Fourier central slice theorem* states that the projection  $p_{\theta_i}$ , of the volume  $v$  in the direction  $\theta_i$ , is the inverse Fourier transform of the slice through  $V = \mathcal{F}v$  in the corresponding direction [6]. We model this theorem by using the matrix  $\mathbf{M}_{\theta_i}$ , which masks the slice, and the rotation matrix  $\mathbf{R}_{\theta_i}$ , which rotates the masked volume into a 2D plane:

$$p_{\theta_i} = Proj(v, \theta_i) = \mathcal{F}^{-1}(\mathbf{R}_{\theta_i}(\mathbf{M}_{\theta_i} \odot V)). \quad (2)$$

The *direct Fourier reconstruction method* calculates the volume  $\tilde{v}$ , a reconstruction of the volume  $v$  from  $p_{\Theta}$ , a set of  $k$  projections  $p_{\theta_i}$ . Our approach defines a matrix  $\mathbf{W}_{\Theta} = (\sum \mathbf{M}_{\theta_i})^{-1}$ , and applies it in Fourier space to calculate the reconstruction:

$$\tilde{v} = Rec(p_{\Theta}) = \mathcal{F}^{-1} \left( \mathbf{W}_{\Theta} \odot \left( \sum_i^k (\mathbf{R}_{\theta_i}^{-1} \mathcal{F}(p_{\theta_i})) \right) \right). \quad (3)$$

If the Fourier space is fully sampled then  $\mathbf{W}_{\Theta}$  is well-defined. Additionally, if it is sampled uniformly,  $\mathbf{W}_{\Theta}$  can be found analytically, and it takes the form of the *ramp filter* [7]:  $\mathbf{W}_{\Theta} = \frac{1}{|w|}$ ; if not,  $\mathbf{W}_{\Theta}$  has to be calculated numerically according to the geometry of the projections [8]. In limited angle tomography the Fourier space is not fully sampled and Eq. 3 becomes an ill-posed problem. In this case, the reconstruction method only finds an approximation of the original volume, and regularization techniques are used to enhance the reconstruction quality and minimize the artifacts [9], [10], [11]. In our case, we will not reconstruct a volume but the cross-correlation between two volumes, which has the property of being sparse when the two volumes are similar.

Let  $\tilde{v} = Rec(p_{\Theta})$  be a limited angle tomogram, and  $v$ , a reference volume, then a projection of the cross-correlation

$\varphi_{\tilde{v}, v} = \mathcal{F}^{-1}(\mathcal{F}\tilde{v} \odot \overline{\mathcal{F}v})$  in the direction  $\theta_i$  is:

$$\begin{aligned} \varphi_{\tilde{v}, v}^{(\theta_i)} &= Proj(\varphi_{\tilde{v}, v}, \theta_i) \\ &= \mathcal{F}^{-1}(\mathbf{R}_{\theta_i}(\mathbf{M}_{\theta_i} \odot (\tilde{V} \odot \bar{V}))) \\ &= \mathcal{F}^{-1}(\mathbf{R}_{\theta_i}(\tilde{V} \odot (\mathbf{M}_{\theta_i} \odot \bar{V}))) \\ &= \mathcal{F}^{-1}(\mathbf{R}_{\theta_i}((\mathbf{R}_{\theta_i}^{-1} P_{\theta_i}) \odot (\mathbf{M}_{\theta_i} \odot \bar{V}))) \\ &= \mathcal{F}^{-1}(P_{\theta_i} \odot \mathbf{R}_{\theta_i}(\mathbf{M}_{\theta_i} \odot \bar{V})) \\ &= \mathcal{F}^{-1}(\mathcal{F}p_{\theta_i} \odot \overline{\mathcal{F}Proj(v, \theta_i)}) \\ &= \varphi_{p_{\theta_i}, Proj(v, \theta_i)}. \end{aligned} \quad (4)$$

Equation 4 shows that the projection of the cross-correlation  $\varphi_{\tilde{v}, v}$  in the direction  $\theta_i$  is the cross-correlation between the projections of  $\tilde{v}$  and  $v$  in the corresponding direction. Following this result, we can reconstruct  $\varphi_{\tilde{v}, v}$  from a set of projections  $p_{\Theta}$ , as we suggested previously [12]. Let  $p_{\Theta}$  be a set of 2D projections of  $\tilde{v}$ , and  $v$ , a 3D volume used as a reference, then the cross-correlation  $\varphi_{\tilde{v}, v}$  can be calculated by reconstructing a set of 2D cross-correlations between each projection  $p_{\theta_i}$  and a corresponding projection of  $v$ :

$$\varphi_{\tilde{v}, v} = Rec(\varphi_{p_{\Theta}, Proj(v, \Theta)}). \quad (5)$$

We must note that the cross-correlation function takes the form of a *delta Dirac* function when the two volumes are mostly similar. We can use this knowledge to enhance the reconstruction of  $\varphi_{\tilde{v}, v}$  by adding the  $l_1$  penalty. Then, to calculate the cross-correlation we must solve:

$$\underset{\varphi_{\tilde{v}, v}}{\operatorname{argmin}} \|\| Proj(\varphi_{\tilde{v}, v}, \Theta) - \varphi_{p_{\Theta}, Proj(v, \Theta)} \|_2^2 + \|\varphi_{\tilde{v}, v}\|_1 \quad (6)$$

Solving equation 6 involves the reconstruction of  $\varphi_{\tilde{v}, v}$  multiple times. To save computation time we rewrite it as an enhancing procedure instead of a reconstruction, then, the enhanced cross-correlation  $\varphi^*$  is calculated by solving:

$$\underset{\varphi^*}{\operatorname{argmin}} \|\|\varphi^* - \varphi_{\tilde{v}, v}\|_2^2 + \|\varphi^*\|_1. \quad (7)$$

We use the Alternating Direction Method of Multipliers (ADMM) to solve it [13]. Let  $\mathcal{S}_{\lambda}()$  be the *shrinkage* function as defined for the ADMM,  $\lambda$ , the regularization parameter, and  $\rho$ , the fidelity coefficient; then the formulas for the ADMM iteration are:

$$x^{j+1} = \frac{\varphi_{\tilde{v}, v} + \rho(z^j - u^j)}{1 + \rho} \quad (8)$$

$$z^{j+1} = \mathcal{S}_{\lambda}(x^{j+1} + u^j) \quad (9)$$

$$u^{j+1} = u^j + x^{j+1} - z^{j+1} \quad (10)$$

The *projected cross-correlation (pCC)*, defined in equation 5, and the *regularized projected cross-correlation (pCC\_reg)*, defined in equation 7, are the foundations of the proposed method for alignment of limited angle tomograms. They lower the computational complexity of the cross-correlation from  $O(N^3)$  to  $O(kN^2)$  for the computationally intensive operations. The reconstruction part is the only  $O(N^3)$  operation, but its computational complexity can be lowered if we know the maximal range of shifts between the volumes. In this case,

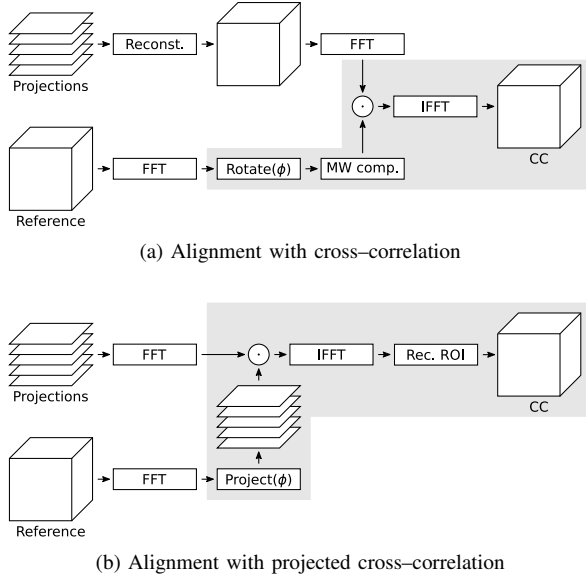


Fig. 1. Comparison of alignment methods for volumes. The operations over the gray background are repeated multiple times for different values of  $\phi$ . These schemes show that the proposed method works mainly with a set of 2D projections instead of 3D volumes.

we replace the full reconstruction part with a localized one with lower computational complexity, which also reduces the number of operations of the ADMM iteration.

### III. ALIGNMENT FOR LIMITED ANGLE TOMOGRAPHY

The current procedure to align a pair of volumes involves the exhaustive search of orientation and shifts which maximizes the cross-correlation between the aligned volumes. Given a set of possible orientations  $\Phi$ , the reference volume  $v$  is transformed to Fourier space and rotated  $\phi \in \Phi$  degrees. Then, the artifacts from the limited angle tomograms are compensated and the cross-correlation is calculated (Fig. 1a). As we mentioned before, the Fourier transform of a limited angle tomogram is sparse and we can use the  $pCC$  (Equation 5) [12] or the  $pCC_{reg}$  (Equation 7) to speed up the alignment.

It is straight forward to demonstrate that the rotation of the reference volume can be embedded in the projection procedure. With this in mind, the newly proposed method of alignment of volumes starts by projecting the reference volume  $v$  in the direction of  $\phi_{\Theta}$  (where  $R_{\phi_{\Theta}} = R_{\phi}R_{\Theta}$ ). Each projection is cross-correlated with its corresponding projection  $p_{\theta_i}$ , and a region of interest for 3D cross-correlation is reconstructed using the localized algorithm (Fig. 1b). We named this method *Substack (alignment and) Averaging (SsA)*, as in it works with stacks (set of projections) instead of subtomograms.

A key part of SsA is the usage of a fast localized reconstruction algorithm. Our implementation uses Algorithm 1, a *weighted back projection* algorithm [7] where the weights are applied in Fourier space and the reconstruction is done in real space only in a Region of Interest (ROI). This algorithm can be accelerated by GPUs, as each value of the cross-correlation

is calculated independently and the interpolation functions can be implemented using the texture memory on the GPU.

---

#### Algorithm 1: Localized Reconstruction (Rec\_ROI)

---

**Input** :  $P_{\Theta}$ , a set of  $K$  projections in Fourier space;  
 $\Theta$ , a set of  $K$  angles;  
 $c_L$ , a set of  $L$  coordinates (ROI).

**Output**:  $rec$ , the reconstruction on the ROI.

```

 $rec \leftarrow 0$ ;
 $W \leftarrow \text{CreateRampFourierSpace}()$ ;
 $p \leftarrow \mathcal{F}^{-1}(W \odot P_{\Theta})$ ;
for  $l \leftarrow 1$  to  $L$  do
    for  $i \leftarrow 1$  to  $K$  do
         $rec[l] \leftarrow rec[l] + \text{Interp}(p_i, \mathbf{R}_{\theta_i} c_L[l])$ ;
    
```

---

#### A. Substack Alignment and Averaging (SsA)

The subtomogram averaging method (StA) [3] consist of two steps: aligning a large set of volumes, or subtomograms, against a reference; and averaging the subtomograms to obtain a high SNR volume. The proposed method, the Substacks Alignment and Averaging (SsA), aligns a set of projections, or substacks, to a reference volume, and uses the *direct Fourier reconstruction method* [8] to obtain the final volume. The alignment part is computational intensive for both StA and SsA, but the usage of the *projected cross-correlation (pCC)* lowers the execution time dramatically for the later.

Algorithm 2 describes the alignment procedure of the SsA method. It uses *regularized projected cross-correlation*, which can be enabled or disabled by setting the value of  $I$ , the number of ADMM iterations. In a similar way to Algorithm 1, the alignment may be accelerated on GPU. Most of the operations work in an element-wise fashion, including the ADMM part. Additionally, the function  $Max()$  and  $ArgMax()$  can be implemented using atomic operations; this way  $rec_{\phi}$ ,  $x$ ,  $u$  and  $z$  can be stored in registers instead of shared or global memory. The algorithm is simple and easy to implement.

### IV. EXPERIMENTAL RESULTS

We performed two computational experiments in order to evaluate the performance of our proposed algorithms. First, we verify the accuracy of the angular search procedure using  $pCC$  and  $pCC_{reg}$ , and we compare the results with two reference algorithms: PBVA and StA. In the second experiment, we compare the execution times of the two proposed algorithms and the current implementation of StA.

The cross-correlation algorithms were implemented in MATLAB R2018b and optimized using MEX interfaces for C/C++ code. A prototype of the SsA method was implemented also in MATLAB, using the Parallel Computing Toolbox to call CUDA subroutines. All the tests were executed on a workstation equipped with an Intel Xeon E5-2630 CPU (16 physical cores, 2MB cache memory), 158GB of RAM memory, 7 GeForce GTX TITAN-X (12GB RAM) GPUs, and running CentOS Linux 7.4.

The reference volume used for the experiments is a Leishmania ribosome bound to paromomycin (PDB 6AZ1), originally solved using *single particle cryo-EM* [14]. The volume

**Algorithm 2: Substack Averaging: Alignment**


---

```

Input :  $p_\Theta$ , a set of  $K$  2D projections;
          $v$ , a reference volume;
          $c_L$ , a set of  $L$  coordinates (ROI);
          $\Phi$ , a set of angles (angular search);
          $I, \lambda, \phi$ , optional ADMM parameters.
Output:  $\phi^*, t^* = \operatorname{argmax}_{\phi, t} \{\varphi_{p_{\theta_i}, v}\}$ 

 $\phi^* \leftarrow 0; t^* \leftarrow 0, m_\phi \leftarrow 0;$ 
 $P_\Theta \leftarrow \mathcal{F}p_\Theta; V \leftarrow \overline{\mathcal{F}v};$ 
foreach  $\phi \in \Phi$  do
  /* projected cross--correlation */
   $V_{\phi_\Theta} \leftarrow \operatorname{Proj}(V, \phi_\Theta);$ 
   $rec_\varphi \leftarrow \operatorname{RecROI}(P_\Theta \odot V_{\phi_\Theta}, \phi_\Theta, c_L);$ 
  /* ADMM (optional) */
  if  $I > 0$  then
     $x \leftarrow 0; u \leftarrow 0; z \leftarrow 0;$ 
    for  $i \leftarrow 1$  to  $I$  do
       $x \leftarrow \frac{rec_\varphi + \rho(z - u)}{1 + \rho};$ 
       $z \leftarrow \operatorname{Shrink}(x + u);$ 
       $u \leftarrow u + x - z;$ 
     $rec_\varphi \leftarrow x;$ 
  /* update output values */
   $m_\varphi \leftarrow \operatorname{Max}(rec_\varphi);$ 
  if  $m_\varphi > m_\phi$  then
     $m_\phi \leftarrow m_\varphi; t^* \leftarrow \operatorname{ArgMax}(rec_\varphi); \phi^* \leftarrow \phi;$ 

```

---

has a size of  $384^3$  voxels, with a voxel size of  $1.05^3 \text{ \AA}$ , with a reported resolution of  $2.7 \text{ \AA}$ . It was resized to a  $120^3$  volume for the first experiment, and to multiple volume sizes for the second one. Each volume was projected in 187 different orientations to obtain the substack datasets for the SsA, and then reconstructed to get the subtomogram datasets for the StA. The projection procedure followed two typical tilting schemes in CryoET: 41 and 61 projections ( $k = 41, k = 61$ ), from  $-60^\circ$  to  $+60^\circ$  in both cases, with  $3^\circ$  and  $2^\circ$  steps, respectively. Additionally, we tested different unconventional tilting schemes to evaluate the effect of the missing views. Subtomogram were generated from the corresponding substacks using a traditional weighted back-projections algorithm.

**A. Test 1: detecting optimal alignment parameters**

In this test, we used the proposed  $pCC$  and  $pCC_{reg}$  algorithms to perform the angular search. As reference algorithms we used the *Projection-Based Volume Alignment (PBVA)* [4], which uses an approximation of  $\varphi$ ; and the alignment by cross-correlation implemented in *Dynamo* [3]. The angular search tests different orientations with an initial angular resolution of  $7.5^\circ$ , to a final resolution of  $0.94^\circ$ . And, besides using different tilting schemes, we corrupted the projections with different levels of Gaussian noise.

The result of the experiment (Table I) shows that the  $pCC$  and  $pCC_{reg}$  have higher alignment precision than the already accurate cross-correlation, which leads to better reconstructions (Fig. 2). The difference is higher when the tilting schemes promotes larger *missing wedges* ( $-40:5:40$  or  $-36:3:36$ ), or when the SNR is low. These three algorithms have a maximum error closer to or lower than the finer angular search step used. On the other hand, the PBVA has a larger

TABLE I  
ANGULAR ERROR OF PARTICLES ORIENTATIONS ESTIMATED BY DIFFERENT ALGORITHMS (IN DEGREES, THE LOWER THE BETTER).

k	Tilting	SNR	CC		pCC		pCC <sub>reg</sub>		PBVA	
			mean	max	mean	max	mean	max	mean	max
17	-40:5:40	-37dB	0.21	1.0	0.15	1.0	0.14	1.0	0.43	3.4
		-55dB	0.29	1.3	0.17	1.0	0.17	1.0	0.42	3.4
		-61dB	0.44	1.3	0.26	1.0	0.27	1.0	0.45	3.5
	-64:8:64	-36dB	0.14	0.9	0.14	0.9	0.14	0.9	0.38	2.4
		-55dB	0.25	0.8	0.17	0.8	0.17	0.8	0.41	2.4
		-61dB	0.45	1.3	0.30	1.0	0.30	1.0	0.46	2.4
	-88:11:84	-36dB	0.17	0.9	0.14	0.8	0.14	0.8	0.38	1.9
		-55dB	0.31	1.0	0.16	0.8	0.17	0.8	0.39	2.4
		-61dB	0.35	2.9	0.28	1.0	0.28	1.0	0.44	3.6
25	-36:3:36	-36dB	0.22	1.0	0.14	1.0	0.14	1.0	0.45	3.5
		-53dB	0.28	1.0	0.15	1.0	0.16	1.0	0.48	3.5
		-59dB	0.41	1.4	0.24	1.0	0.26	1.0	0.50	3.5
	-60:5:60	-35dB	0.14	0.9	0.14	0.9	0.14	0.9	0.38	1.9
		-53dB	0.23	0.9	0.15	0.9	0.15	0.9	0.39	2.4
		-59dB	0.38	1.1	0.24	0.9	0.26	1.0	0.41	2.4
	-84:7:84	-35dB	0.15	0.8	0.14	0.8	0.14	0.8	0.36	2.4
		-54dB	0.25	0.8	0.15	0.8	0.15	0.8	0.39	2.4
		-60dB	0.37	1.0	0.24	1.0	0.25	1.0	0.43	2.9
41	-60:3:60	-34dB	0.14	0.9	0.14	0.9	0.14	0.9	0.38	1.9
		-51dB	0.18	0.8	0.15	0.9	0.14	0.9	0.39	2.1
		-57dB	0.31	0.9	0.20	0.9	0.20	0.9	0.43	3.4
61	-60:2:60	-34dB	0.14	0.9	0.14	0.9	0.14	0.9	0.39	1.9
		-49dB	0.19	0.9	0.14	0.9	0.15	0.9	0.37	1.9
		-55dB	0.29	0.9	0.18	0.9	0.18	0.8	0.40	2.7

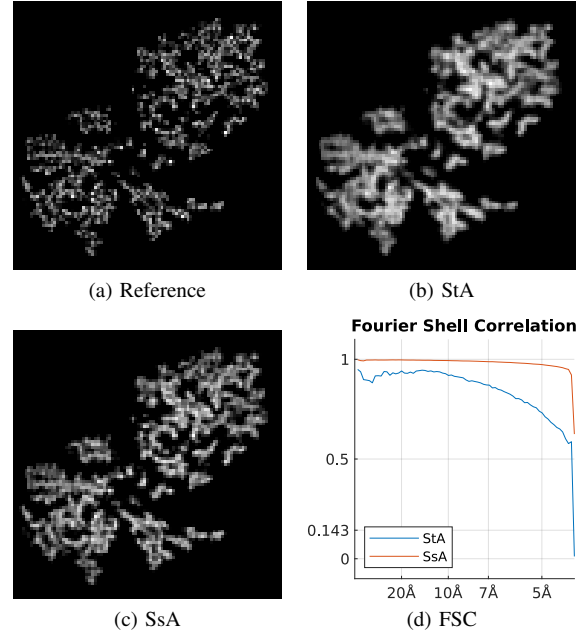


Fig. 2. Comparison of a central slice of 3D reconstructions. (a) Reference volume [14]. (b) Conventional StA reconstruction. (c) Reconstruction using SsA. (d) Fourier Shell Correlation between the reference and the reconstructions.

alignment error, with maximum error values up to four times larger than the finer angular search step used.

**B. Test 2: computational performance on GPU**

In this test we compare the execution time of the alignment part of the subtomogram averaging (StA) and the proposed substacks averaging (SsA). We use the software package *Dynamo* [3] as the reference implementation of the StA, as

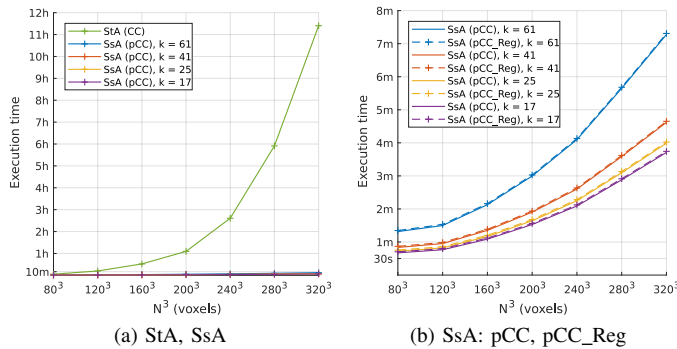


Fig. 3. Comparison of the execution time between Subtomogram Averaging (StA) and the proposed Substack Averaging (SsA) algorithm. 187 particles were aligned using 7 GPUs. The StA implementation uses cross-correlation [3] while the SsA uses the proposed  $pCC$  and  $pCC\_Reg$  algorithms.

it is widely used by the CryoET community. It was written in MATLAB, C++ and CUDA, and it uses the GPUs to speed up the alignment process. Our prototype implementation of the proposed SsA method uses the same languages and also uses the GPUs. As the performance of the SsA depends on the number of projections, we report the execution time in function of  $k$  instead of the tilting schemes.

The execution time for StA grew rapidly from minutes to hours with increasing the box size (Fig. 3), while SsA method kept it in the range of minutes ( $< 8min$ ). This results in a substantial speed up, especially for larger boxes, where the SsA is 92 times faster than the StA, for  $k = 61$ , and up to 146 times faster, for  $k = 17$ . The speed up follows the theoretical reduction of computational complexity of alignment, from  $O(N^3)$ , using cross-correlation, to  $O(kN^2)$ , using the proposed  $pCC$  and  $pCC\_reg$ . Additionally, the usage of ADMM barely increased the execution time.

## V. CONCLUSIONS

In this document we presented the *projected cross-correlation* ( $pCC$ ), and an enhanced version of it, the *regularized projected cross-correlation* ( $pCC\_reg$ ), alternative ways to calculate the cross-correlation. Using them, we develop a fast alignment algorithm for limited angle tomography, which aligns the subtomograms using substacks instead of the subtomogram itself. This lowers the computational complexity of the alignment algorithm from  $O(N^3)$  to  $O(kN^2)$ , where  $k$  is the number of projections. Experimental results confirms that using  $pCC$  yields the same precision of alignment as using the conventional cross-correlation (Table I) but at a significantly increased speed.

$pCC$  and  $pCC\_reg$  have the same accuracy, but the later has higher precision, as its cross-correlation peak is sharper (Fig. 4). Even though it does not improve the alignment accuracy, the  $pCC\_reg$  can be used in the *branch-and-bound* approach for angular search [15] to reduce the number of angles to evaluate. This approach iteratively uses smaller angular steps on a set of angles defined by the *best* angles of the previous iteration.

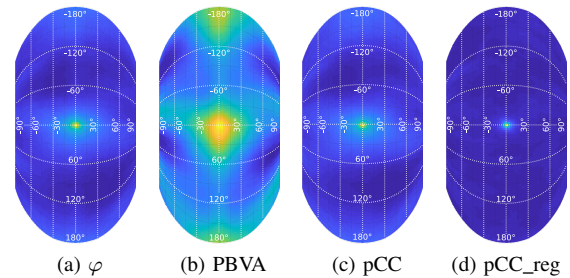


Fig. 4. Example of the angular search results for the alignment of one subtomogram/substack. The cross-correlation ( $\varphi$ ) and the  $pCC$  are equivalent, while the  $pCC\_reg$  has a higher precision. In the other hand, the PBVA shows acceptable accuracy but lower precision.

## ACKNOWLEDGMENTS

Ricardo M. Sánchez and Mikhail Kudryashev are funded by the Sofja Kovalevskaja Award from the Alexander von Humboldt Foundation to Mikhail Kudryashev. Ricardo M. Sánchez is partially supported by the starter Fellowship from SFB807.

## REFERENCES

- [1] V. Lučić, A. Rigort, and W. Baumeister, “Cryo-electron tomography: the challenge of doing structural biology in situ,” *The Journal of cell biology*, 2013.
- [2] J. G. Galaz-Montoya and S. J. Ludtke, “The advent of structural biology in situ by single particle cryo-electron tomography,” *Biophysics Reports*, 2017.
- [3] D. Castaño-Díez, M. Kudryashev, M. Arheit, and H. Stahlberg, “Dynamo: A flexible, user-friendly development tool for subtomogram averaging of cryo-em data in high-performance computing environments,” *Journal of Structural Biology*, 2012.
- [4] L. Yu, R. R. Snapp, T. Ruiz, and M. Radermacher, “Projection-based volume alignment,” *Journal of Structural Biology*, 2013.
- [5] P. Misra, H. W. M. Yang, M. Duarte, and S. Jha, “Sparsity based efficient cross-correlation techniques in sensor networks,” *IEEE Transactions on Mobile Computing*, 2017.
- [6] D. H. Garces, W. T. Rhodes, and N. M. Peña, “Projection-slice theorem: a compact notation,” *Journal of the Optical Society of America. A, Optics, image science, and vision.*, 2011.
- [7] P. A. Penczek, “Fundamentals of three-dimensional reconstruction from projections,” *Methods in Enzymology*, 2010.
- [8] J. G. Pipe and P. Menon, “Sampling density compensation in mri: Rationale and an iterative numerical solution,” *Magnetic Resonance in Medicine*, 1999.
- [9] P. C. Hansen and J. H. Jørgensen, “Total variation and tomographic imaging from projections,” in *Thirty-Sixth Conferenc of the Dutch-Flemish Numerical Analysis Communities*, 2011.
- [10] J. Dong-Jiang, H. Wen-Zhang, and Z. Xiao-Bing, “Tv os-sart with fractional order integral filtering,” in *Eight International Conference on Computational Intelligence and Security*, 2012.
- [11] J. Friel, “Sparse regularization in limited angle tomography,” *Applied and Computational Harmonic Analysis*, 2013.
- [12] R. M. Sanchez, R. Mester, and M. Kudryashev, “Fast cross correlation for limited angle tomographic data,” in *Image Analysis. SCIA 2019. Lecture Notes in Computer Science*, 2019.
- [13] S. Boyd, N. Parikh, E. Chu, B. Peleato, and J. Eckstein, “Distributed optimization and statistical learning via the alternating direction method of multipliers,” *Foundation and Trends in Machine Learning*, 2011.
- [14] M. Shalev-Benami, Y. Zhang, H. Rozenberg, Y. Nobe, N. Taoka, D. Matzov, E. Zimmerman, A. Bashan, T. Isobe, C. L. Jaffe, A. Yonath, and G. Skiniotis, “Atomic resolution snapshot of leishmania ribosome inhibition by the aminoglycoside paramomycin,” *Nature Communications*, 2017.
- [15] A. Punjani, J. L. Rubinstein, D. J. Fleet, and M. A. Brubaker, “cryosparc: algorithms for rapid unsupervised cryo-em structure determination,” *Nature Methods*, 2017.